# EFFECT OF SURFACE ROUGHNESS ON SERS ENHANCEMENT OF PATTERNED GOLD SUBSTRATES

**István Rigó[1*], Miklós Veres[1], Tamás Váczi[1], Zsolt Zolnai[2], Rebeka Öcsi[2], Péter Fürjes[2]**

*[1]Institute for Solid State Physics and Optics, Wigner Research Centre for Physics, ELKH, 1121 Budapest, Konkoly-Thege Miklós way 29-33, Hungary*
*[2]Institute of Technical Physics and Materials Science, Centre for Energy Research, ELKH, 1121 Budapest, Konkoly-Thege Miklós way 29-33, Hungary*
**e-mail: rigo.istvan@wigner.hu*

## 1. INTRODUCTION

Raman spectroscopy is a non-contact, fast, and relatively easy material characterization technique requiring no sample preparation. It is finding many applications in biology, life sciences, and other areas. While Raman scattering is inherently weak (its cross-section can be orders of magnitude smaller than that of fluorescence [Kumar 2012]), the sensitivity of the method can be improved remarkably by implementing surface-enhanced Raman scattering (SERS) [Ryder 2005], where the degree of achievable sensitivity can reach up to attomolar ($10^{-18}$ M) concentrations [Kneipp 1997, Etchegoin 2003]. As a spectroscopic tool, SERS has the potential to combine the sensitivity of fluorescence with the structural information given by Raman spectroscopy.

During SERS the scattering takes place in close vicinity of nanostructured metallic surfaces [Li 2017]. The interaction of the electromagnetic field of photons with the surface plasmons of the metallic nanostructure results in the enhancement of the Raman signal; the gain of which can be several orders of magnitude. A successful SERS experiment requires an appropriate SERS-active agent (in most cases, nanoparticles or substrates) that will provide the required efficiency at a given excitation wavelength.

Periodic arrays of inverse pyramids with characteristic size of a few micrometers were among the first SERS active substrates finding commercial utilization [Stokes 2010]. Recently we found that the insertion of a gold nanoparticle (GNP) into the inverse pyramid remarkably increases the near-field enhancement (NFE) properties of the structure. Our results showed that the near-field intensity distribution depends on the size of the nanoparticle [Rigó 2020].

The NFE of the inverse pyramid array can further be improved by introducing nano-roughness to the gold surface. This can be achieved for example, by laser ablation altering the surface morphology of the array. Some preliminary experiments with a nanosecond laser having high pulse energy have already been performed by our group in this direction. In this work, the effect of the surface treatment on the near-field intensity distribution in inverse pyramids was studied by Finite-difference time-domain (FDTD) calculations and compared with those obtained for the GNP containing system.

The dimensions of the inverse pyramid and the surface roughness were taken from experimental data obtained on real gold coated substrates.

## 2. MATERIALS AND METHODS

SERS substrates were prepared by lithographic technique. A 2×2 micron base has been designed for the inverse pyramids. After the mask formation anisotropic etching was applied to the surface resulting in voids with sharp edges (inverse pyramids). After that the surface was coated with a 150 nanometers thick layer of gold (**Figure 1.**).

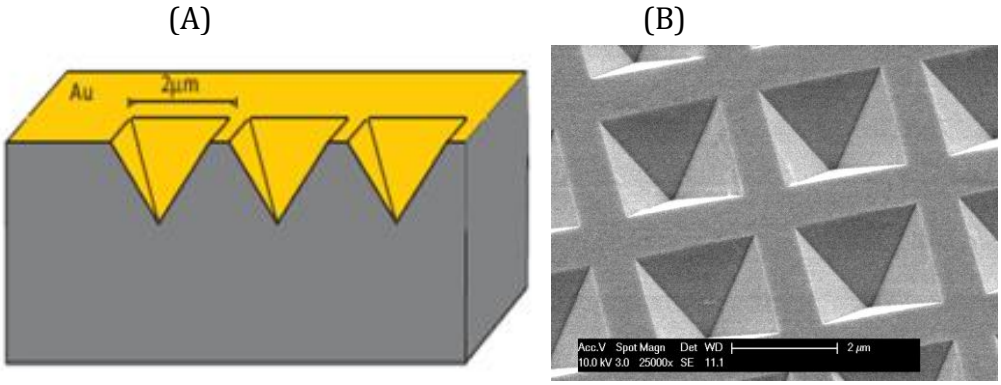


***Figure 1.*** (A) Schematic representation and (B) SEM image of gold coated periodic array of inverse pyramids.

The dimensions of the voids were determined from 3D surface profiles. **Figure 2.** shows a depth profile of the pyramids. It can be seen that due to over-etching the base is 2.9 microns, and the depth of the voids is close to 1.5 microns.

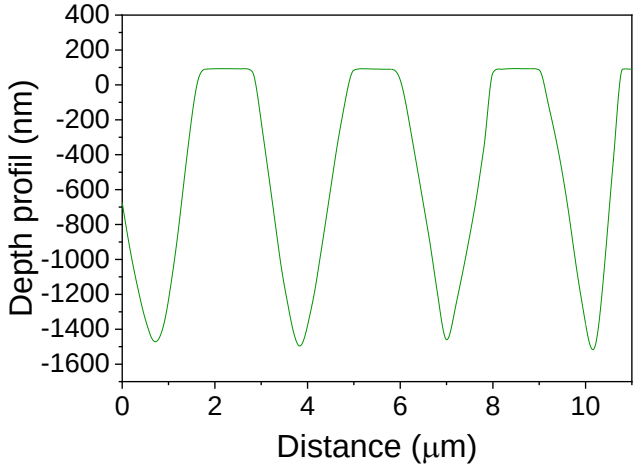


***Figure 2.*** Depth profile of the inverse pyramid array along diagonals.

Near-field intensity distributions of the substrates were studied using the Lumerical FDTD Solutions v.8.15.736 software. Periodic boundary conditions were chosen in the directions parallel to the substrate surface to model the array geometry,

together with perfectly matched layer boundary conditions in the perpendicular direction. The size of the simulation cell was set according to the geometry of the fabricated array structure to 2.9 x 2.9 x 4.6 μm (**Figure 3.**). Silicon was selected as substrate material and a 150 nm gold coating was placed on that. The software's built in material parameter set from CRC Handbook of Chemistry and Physics [Weast 1988] was used for the gold layer and that from the Handbook of Optical Constants of Solids I [Palik 1998], for the silicon substrate. The simulation grid was defined by the built-in auto mesh algorithm with an accuracy level of 3 and 4. The inverse pyramid array was illuminated using a broad band (400–900 nm) plane wave having normal incidence to the array surface and polarization parallel to the base of the pyramid. Near-field profiles were recorded using two monitors placed along the two symmetry planes of the pyramid XZ and YZ plane, being perpendicular, and a third one XY placed above and being parallel to the array surface.

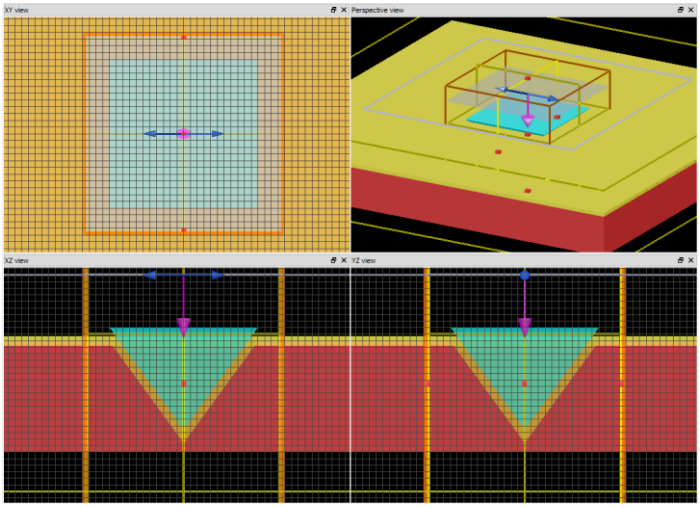

***Figure 3.*** FDTD model geometry used for calculations.

The surface roughness has been introduced into the model by creating a rough surface with given RMS amplitude and correlation length, and 'wrapping' it to create the shape. The roughness was generated by generating a random matrix of values in K-space. A Guassian filter was applied to this matrix, then a Fourier transformation (FT) was used to transform the matrix back to real space. The FT parameters were selected so that the roughness had periodicity in the X and Y directions corresponding to the void model dimensions. This was necessary to avoid seaming during the wrapping of the rough surface.

## 3. RESULTS AND DISCUSSION

**Figure 4.** compares the calculated near-field intensity (E) distributions of empty and GNP containing pyramids together with the structure having surface roughness in the two monitor planes placed along two symmetry planes of the model structures. It should

be noted that the intensity distribution maps of different structures are not comparable directly since each map has its own intensity scale, shown by the color bars.

It can be seen that the near-field maximum is localized in the lower half of the empty pyramid. The data obtained for the 50 nm and 100 nm samples are very similar to the empty pyramid, including the near-field intensity distributions and even the magnitudes. For the 100 nm sample local fields of small intensity can also be observed at the bottom of the void, around the gold nanoparticle. The intensity map of the structure with rough surface is differs mainly in the expansion of the region with high intensity compared to the empty, 50 or 100 nm GNP. In addition, it shows the largest values.

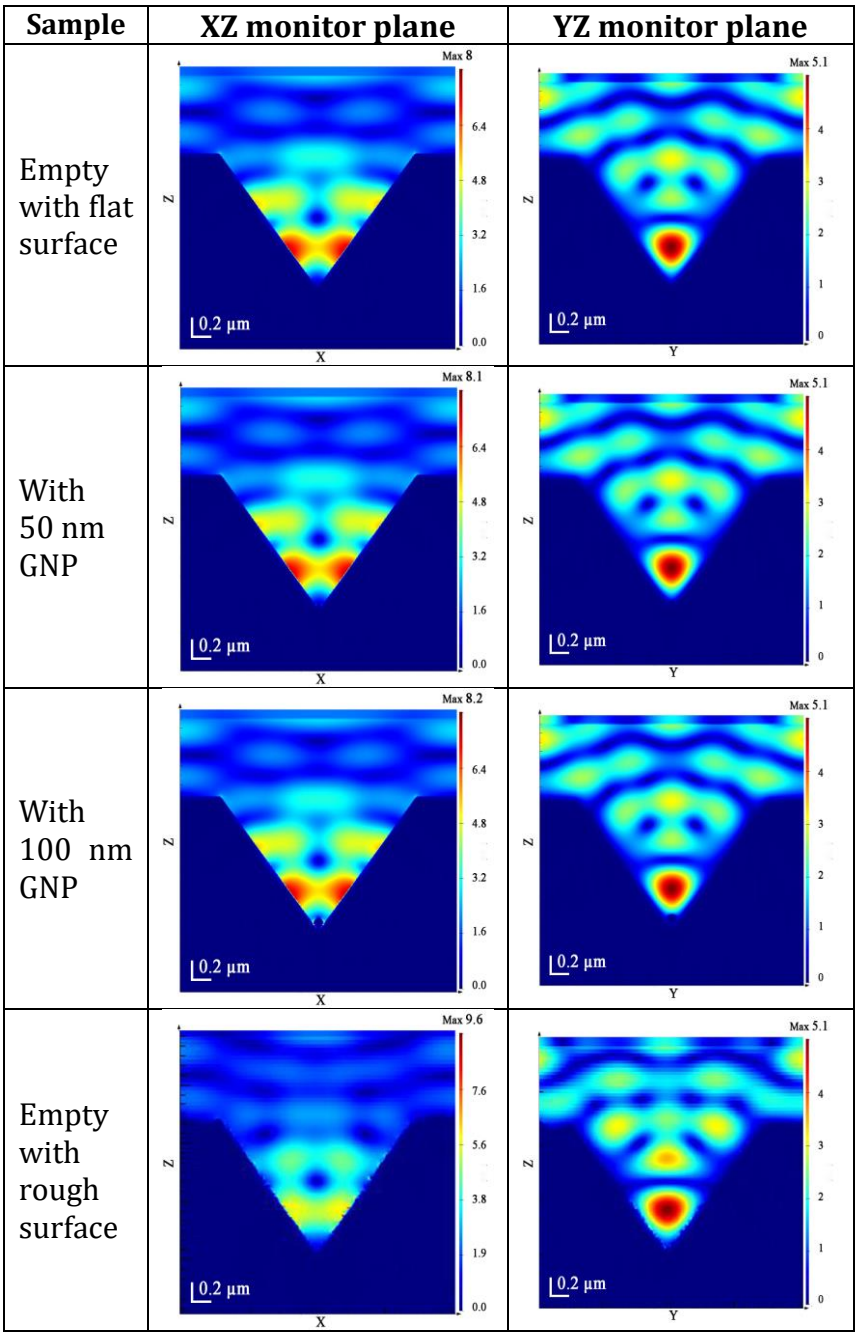


***Figure 4.*** Calculated distributions of near-field intensity (E) inside the empty inverse pyramid with flat and rough surfaces, and that entrapping a 50 and 100 nm gold nanosphere.

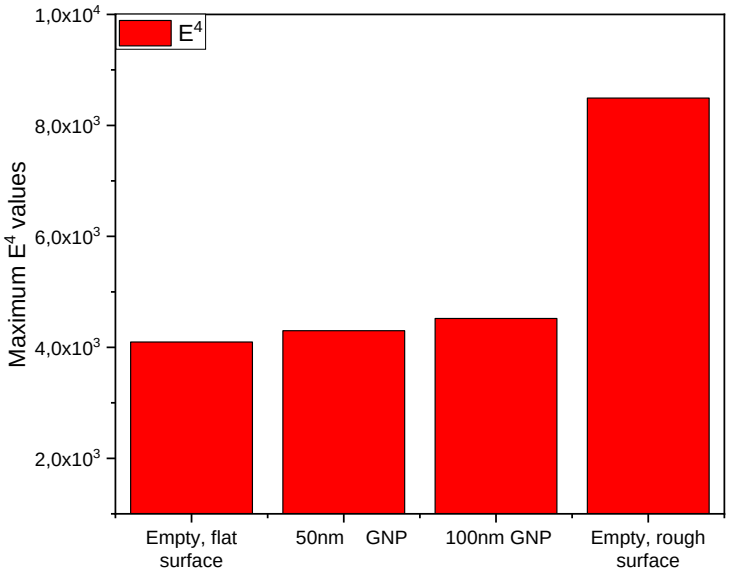


***Figure 5.*** Maximum $E^4$ values obtained from calculated near-field intensity distributions.

Since surface enhanced Raman scattering and fluorescence scale approximately as $E^4$ [Pilot 2019], the maximum $E^4$ values were obtained for the samples with different GNPs and the surfaces (**Figure 5.**). As it can be expected from the intensity distribution maps above, the flat surface empty, 50 nm and 100 nm samples have similar $E^4$ values around 4-5 x $10^3$. However, the empty pyramid with rough surface is close to $10^4$.

## 4. CONCLUSIONS

Near-field intensity distributions were determined by FDTD calculations for micrometer-sized gold coated inverse pyramids with flat and rough surface, and with entrapped 50 nm and 100 nm gold nanoparticles. The maximum $E^4$ values were also determined. It was found that the addition of gold nanoparticles into the void increases the maximum of near filed intensity, and so the near-field enhancement properties of these structures. However, fabrication of structures with rough surfaces on the nanoscale level is even more efficient. Its theoretical near-field enhancement factor was found to be almost $10^4$.

## 5. ACKNOWLEDGEMENTS

This work was supported by the VEKOP-2.3.2-16-2016-00011 grant, which is co-financed by the European Union and European Social Fund.

## 6. REFERENCES


[Etchegoin 2003] P. Etchegoin, R. C. Maher, L. F. Cohen, H. Hartigan, *Chem. Phys. Lett.*, 375 (2003) 84.

[Kneipp 1997] K. Kneipp, Y. Wang, H. Kneipp, L. T. Perelman, I. Itzkan, R. R. Dasari, M. S. Feld, *Phys. Rev. Lett.*, 78 (1997) 1667.

[Kumar 2012] C. S. S. R. Kumar: Raman spectroscopy for nanomaterials characterization, *Springer-Verlag,* 2012.

[Li 2017] W. Li, X. Zhao, Z. Yi, A. M. Glushenkov, L. Kong, *Anal. Chim. Acta*, 984 (2017) 41.

[Palik 1998] E. D. Palik: Handbook of Optical Constants of Solids II, *Academic Press,* 1998.

[Pilot 2019] R. Pilot, R. Signorini, C. Durante, L. Orian, M. Bhamidipati, L. Fabris, *Biosensors*, 9 (2019) 57.

[Rigó 2020] I. Rigó, M. Veres, Zs. Pápa, L. Himics, R. Öcsi, O. Hakkel, P. Fürjes, *J. Quant. Spectrosc. Radiat. Transf.*, 253 (2020) 107128.

[Ryder 2005] A. G. Ryder, *Curr. Opin. Chem. Biol.*, 9 (2005) 489.

[Stokes 2010] R. Stokes, D. Graham, U.S. Patent Appl. No.12/475,141, Pub. No.US 2010/0028908 A1, 2010.

[Weast 1988] R. C. Weast, M. J. Astle, W. H. Beyer: CRC Handbook of Chemistry and Physics - 69th Edition, *CRC Press*, 1988.